# A Study on Thermal Performance of Heat Pipe for Optimum Placement of Satellite Equipment

Jong Heung Park

## CONTENTS



## ABSTRACT

A study on the operation of a heat pipe with two heat sources has been performed to optimize the heat distribution of satellite equipment. A numerical modeling is used to predict the temperature profile for the heat pipe assuming cylindrical two-dimensional laminar flow for the vapor, and the conduction heat transfer for the wall and wick. An experimental study using the copper-water heat pipe with the length of 0.45 m has been performed to evaluate the numerical model and to compare the temperature distribution at the outer wall for the non-uniform heat distribution. The results on temperature profiles for the heat input range from 29 W to 47 W on each heater are presented. Also the correlation between the heat input and the temperature increase is presented for the optimum distribution on two heaters. The result shows that the outer wall temperature can be controlled by redistribution of heat sources. It is also concluded that the heat source closer to the condenser can carry more heat while maintaining lower temperatures at the outer wall.

## NOMENCLATURES

$A$ area, $m^2$
$c_p$ specific heat at constant pressure, J/(kg K)
$h_{fg}$ latent heat of evaporation, J/kg
$k$ thermal conductivity, W/(m K)
$L$ total length of heat pipe, m
$\dot{m}$ mass flux at the liquid-vapor interface, $kg/(m^2\ s)$
$p$ vapor pressure, $N/m^2$
$p_o$ reference pressure, $N/m^2$
$q$ heat flux, $W/m^2$
$Q$ heat input, W
$r$ radial coordinate, m
$R$ gas constant
$R_o$ outer pipe wall radius, m
$R_v$ vapor region radius, m
$R_w$ wick-wall interface radius, m
$T$ temperature, K
$T_o$ reference temperature, K
$v$ radial velocity, m/s
$w$ axial velocity, m/s
$z$ axial coordinate, m
$\varphi$ porosity
$\mu$ dynamic viscosity of the vapor, kg/(m s)
$\rho$ density, $kg/m^3$

Subscripts
$a$ adiabatic
$c$ condenser
$eff$ effective
$H1$ Heater 1
$H2$ Heater 2
$l$ liquid(working fluid)
$lw$ liquid-saturated wick
$r$ radial direction
$s$ wick solid material or saturation
$v$ vapor
$w$ wall

## I. INTRODUCTION

Due to the heat transport by evaporation and condensation of the working fluid, a heat pipe is an effective but simple device which has a very high thermal conductance. Since 1960's, these devices have been developed, tested and put into operation in various types specially for space applications. With these developments, heat pipes are used in many engineering fields nowadays [1], [2].

According to the change of the working conditions and applications, the heat pipe operation with multiple heat sources has been encountered frequently rather than the conventional heat pipe operation with a single heat source and sink. This operation with multiple heat sources can be observed in space application, where the heat pipes are the major devices for the thermal control of satellite equipment. When the heat dissipating equipment such as high power amplifier, frequency converter, and power supply are mounted in series on a heat pipe embedded in a honeycomb panel, these equipment act as multiple heat sources on the heat pipe. It is obvious that a conventional analytical methodology developed for a heat pipe with a single heat source cannot be applied to the operation with multiple heat sources of non-uniform heat distributions.

Gernert [3] attempted the analysis of heat pipe with multiple heat sources with the use of superposition and the extention of the existing theories for the single evaporator heat pipe. He also conducted

an experiment using a 1.5 m long copper-water heat pipe with the total heat input of 1000 W on five heaters. In the study, the performance of the heat pipe such as the temperature profiles and dryout condition was presented. Faghri and Buchko [4] performed an experimental and numerical study of low temperature heat pipe with multiple heat sources. They suggested a complete mathematical model to predict the performance of the heat pipe, including the conjugate heat transfer and the effect of liquid flow in a wick. In addition, the experimental testing using the 1 m long copper-water heat pipe with the heat input range from 97 W to 200 W on four heaters were performed for the optimization of the heat distribution. In spite of the effort of these studies described above, the correlation between the heat input and the temperature increase for the optimum distribution of heat sources were not available in open literature.

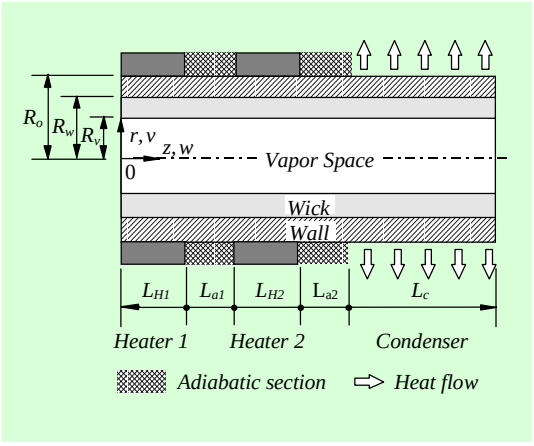


**Fig. 1.** Heat pipe model and coordinate system.

The objective of the present study is to investigate the effect of the heat distribution on the heat pipe performance for the optimum placement of satellite equipment. The temperature prediction by the numerical modeling as well as the experiment with a copper-water heat pipe have been performed. The results on the temperature profiles for the heat input range of 29 W to 47 W on each heater are presented. Also, the correlations between the heat input and temperature increase are presented for the optimum heat distribution on two heaters.

## II. NUMERICAL ANALYSIS

### 1. Mathematical Modeling

Fig. 1 shows the simplified model and the coordinate system of the heat pipe used in the present study, which is a conventional one with two heaters. These heaters can be considered as equivalent satellite equipment which dissipate heat. The heat pipe configuration shown in Fig. 1 can be divided into three regions, namely, vapor space, wick and wall regions. The working fluid is saturated with wick in liquid phase. The power applied to the heaters causes the liquid in the wick to vaporize. The vapor flows to the condenser section and releases the heat as it condenses. The released heat is rejected through the wall to the ambient. The condensed working fluid in the wick returns to Heater 1 and Heater 2 sections by the capillary force of the wick structure.

## 2. Governing Equations

The several numerical methodologies for a heat pipe with multiple heat sources have been developed [5]-[8]. Among them, the modeling from Chen and Faghri [8] is adopted for the present study, which showed a good agree-ment for both high-temperature and low-tem-perature heat pipes. Therefore, the governing equations for this model can be described in three different radial regions. These equations should be solved as a conjugate problem due to the heat and mass flow along the interface.

### A. Vapor Space

Bowman and Hitchcock [9] reported the vapor flow was always laminar in the condenser, while it might be turbulent when the Reynolds number is greater than 2000. According to Dunn and Reay [10], the compressibility of vapor could not be ignored when the Mach number is greater than 0.3. Since the Reynolds number and the Mach number in the present study are approximately 210 and 0.01 respectively, the vapor is assumed to be an incompressible laminar flow. Consequently, the governing equations for the two-dimensional incompressible laminar flow with constant viscosity in the cylindrical r-z coordinate are given as follows [11].

$$\frac{1}{r}\frac{\partial}{\partial r}(rv)+\frac{\partial}{\partial z}(w)=0 \tag{1}$$

$$\frac{1}{r}\frac{\partial}{\partial r}(\rho rv^2)+\frac{\partial}{\partial z}(\rho vw) = -\frac{\partial p}{\partial r}+\mu\left[\frac{\partial}{\partial r}\left(\frac{1}{r}\frac{\partial}{\partial r}(rv)\right)+\frac{\partial^2 v}{\partial z^2}\right] \tag{2}$$

$$\frac{1}{r}\frac{\partial}{\partial r}(\rho rvw)+\frac{\partial}{\partial z}(\rho w^2) = -\frac{\partial p}{\partial z}+\mu\left[\frac{\partial}{\partial r}\left(\frac{1}{r}\frac{\partial}{\partial r}(rw)\right)+\frac{\partial^2 w}{\partial z^2}\right] \tag{3}$$

$$\rho c_p\left(v\frac{\partial T}{\partial r}+w\frac{\partial T}{\partial z}\right)=k\left[\frac{1}{r}\frac{\partial}{\partial r}\left(r\frac{\partial T}{\partial r}\right)+\frac{\partial^2 T}{\partial z^2}\right], \tag{4}$$

where $\rho$, $p$, $\mu$, $c_p$, $T$ and $k$ are density, pressure, viscosity, specific heat, temperature and thermal conductivity of the working fluid in the vapor phase.

### B. Wick

Faghri and Buchko [4] performed an experimental and numerical analysis on a 1.0 m long copper-water heat pipe with the total heat input range of 97 W to 200 W. It was concluded that the effect of the liquid flow in the wick could not be ignored in a low-temperature heat pipe. However, one dimensional calculation of the liquid flow in the wick for the present heat pipe with a 0.45 m in length and heat input range between 58 W to 94 W showed that the axial average velocity in the wick was in the order of $10^{-4}$ m/s, which is relatively low enough to ignore the impact of the liquid flow on the temperature distribution. This does not mean that the flow in the wick is not important. However, in order to save the effort of calculation, the wick flow is ignored in the present study for convenience. In addition, since the calculation of capillary limit suggested by Dunn and Reay [10] was about 300 W used for the present study, the wick structure is assumed to have a sufficient capillary force to avoid the operational failure. Based on

these assumptions, the wick region is modeled as pure conduction with an effective thermal conductivity. The corresponding governing equation is

$$k_{eff}\left[\frac{1}{r}\frac{\partial}{\partial r}\left(r\frac{\partial T_{lw}}{\partial r}\right)+\frac{\partial^2 T_{lw}}{\partial z^2}\right]=0 \qquad (5)$$

where the effective thermal conductivity, $k_{eff}$ is calculated from (6) based on the metal screen wick [10], [12].

$$k_{eff}=\frac{k_l[(k_l+k_s)-(1-\varphi)(k_l-k_s)]}{[(k_l+k_s)+(1-\varphi)(k_l-k_s)]}, \qquad (6)$$

where $\varphi$ is the porosity of the wick and subscripts $l$ and $s$ indicate the working fluid in the wick in liquid phase and the solid material of the screen mesh, respectively.

### C. Wall

The heat transfer through the heat pipe wall is purely by conduction. The corresponding governing equation is

$$k_w\left[\frac{1}{r}\frac{\partial}{\partial r}\left(r\frac{\partial T_w}{\partial r}\right)+\frac{\partial^2 T_w}{\partial z^2}\right]=0. \qquad (7)$$

## 3. Boundary Conditions

Boundary conditions are needed at both ends of the heat pipe, at the centerline, at the vapor-wick interface, at the wall-wick interface, and at the outer wall. At both ends of the heat pipe, the no-slip condition for the velocity and the adiabatic condition for the temperature are applied.

$$v=w=0,\ \frac{\partial T}{\partial z}=0 \quad \text{at} \quad z=0,\ L \qquad (8)$$

At the centerline, the symmetry conditions are applied.

$$\frac{\partial w}{\partial r}=0,\ v=0,\ \frac{\partial T}{\partial r}=0 \quad \text{at} \quad r=0 \qquad (9)$$

At the vapor-wick interface, the temperature is assumed to be at saturation, corresponding to the interface pressure during heat pipe operation. Thus the interface temperature is calculated using the Clausius-Clapeyron equation [12] given by

$$T=\frac{1}{\frac{1}{T_o}-\left(\frac{R}{h_{fg}}\right)ln\left(\frac{p_v}{p_o}\right)} \quad \text{at} \quad r=R_v, \qquad (10)$$

where $R$, $h_{fg}$, $p_o$, and $T_o$ are gas constant, latent heat of the working fluid, reference saturation pressure, and reference temperature, respectively. For the velocity, the boundary conditions are defined based on the rate of evaporation and condensation of the working fluid. The radial and the axial velocities along the vapor-wick interface are given by

$$v_i=\frac{\dot{m}}{\rho}=\frac{q}{\rho h_{fg}}=\frac{1}{\rho h_{fg}}\left(k_v\frac{\partial T_v}{\partial r}-k_{eff}\frac{\partial T_{lw}}{\partial r}\right) \qquad (11)$$
$$w=0 \quad \text{at} \quad r=R_v,$$

where $\dot{m}$ is the mass flux at the vapor-wick interface. According to the coordinate system shown in Fig. 1, interface velocity $v_i$ is negative in the heater section(blowing) and is posi-tive in the condenser section(suction) to balance the mass flow.

At the wick and wall interface, the boundary condition is

$$k_w \frac{\partial T_w}{\partial r} = k_{eff} \frac{\partial T_{lw}}{\partial r} \quad \text{at} \quad r = R_w. \qquad (12)$$

At the outer wall, a constant heat flux boundary is used.

$$k_w \frac{\partial T_w}{\partial r} = \pm \frac{Q}{A} \quad \text{at} \quad r = R_o \qquad (13)$$

The heat flux in [13] is constant and positive in the heater sections, zero in all the adiabatic sections and negative in condenser section based on the uniform distribution of total heat through the heaters.

### 4. Numerical Methodology

The conjugate heat transfer problem should be solved not only because three radial regions with different properties are solved simultaneously, but also because there is heat transfer through the interfaces of the regions. The PHOENICS computational code by Rosten and Spalding [13] which employed the finite-difference method was used to solve the governing equations with the above boundary conditions. The pressure at the vapor-wick interface at the end of the condenser was taken as a fixed datum pressure for the calculation. The phase change at the vapor-wick interface is simply treated as a source term in the energy equation. The latent heat is added as a positive value where the condensation occurs and as a negative value where the evaporation occurs.

The grid consists of 25(radial) by 45(axial). A converged solution is defined as the condition when the difference for the absolute values of dependent variables is less than 0.1 % between two successive iterations and when the sum of the absolute values of residuals is less than $10^{-9}$. A false time step relaxation [13] is used to solve $v$ and $w$ momentum equations.

## III. EXPERIMENT

Because the major objective of this study was to investigate the effect of the heat distribution on the heat pipe performance, it was decided to use a conventional commercial heat pipe for an experiment instead of making a new pipe. The heat pipe selected for the experiment was a copper-water heat pipe(Thermacore Inc., HP-2) which was rated to operate at a temperature range of 40 °C to 180 °C. Table 1 shows the details of the heat pipe. The dimension is 0.45 m in length and 0.0158 m in diameter. The wall and the wick thickness are 0.001 m each. A simple circumferential screen wick consisting of three layers of 100 mesh copper screen wire is installed to provide the working fluid return by capillary force.

The experimental apparatus is shown in Fig. 2. A total of twelve type-T type thermocouples with an accuracy of ±0.5 °C were attached on the outer wall with a thermal bond. Two rubber coated flexible heaters equivalent to satellite equipment were wrapped around the pipe wall. These heaters were independently controlled by a power supply. The length of heaters, $L_{H1}$

**Table 1.** Summary of experimental heat pipe.

| Item | Material and Size |
|---|---|
| Heat pipe wall | Copper |
| Wick material | Copper |
| End cap material | Copper |
| Working Fluid | Distilled water |
| Length | 450 mm |
| Diameter | 15.8 mm |
| Diameter of vapor space | 11.8 mm |
| Screen mesh number | 100 (3 layers) |
| Length of heater | 100 mm each |
| Length of adiabatic section | 50 mm each |
| Length of condenser | 150 mm |

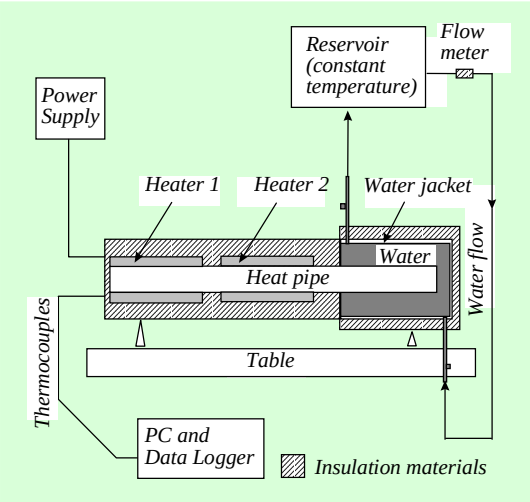


**Fig. 2.** Experimental apparatus.

and $L_{H2}$ was 100 mm each. The length of adiabatic sections, $L_{a1}$ and $L_{a2}$ was 50 mm between heaters and between Heater 2 and condenser section. The entire heat pipe except the condenser section was wrapped by 40 mm thick insulation materials composed of fiber glass and styro-form. Three more thermocouples were placed on the outer surface of the insulation material to measure the heat loss to the surroundings. The net heat input to the heat pipe was defined as the difference between the power input from power supply and the loss through the surface of the insulation material. The loss was about 5 % $\pm$ 1 % in the present apparatus. In the condenser section, the cooling water was circulating in a water jacket made of glass to remove the heat from the condenser. Cooling water was supplied by a pump connected to the constant temperature reservoir which was equipped with a pre-heater to control the water temperature with an accuracy of $\pm$ 0.5 °C. This assembly was mounted horizontally on a work bench. The signals from the thermocouples were read by a thermocouple data logger.

## IV. RESULTS AND DISCUSSIONS

At first, the heat pipe was operated with 38 W heat input at Heater 1 only in order to ensure the proper operation and to establish the temperature setting of cooling water. Figure 3 shows the wall temperature profiles as a function of the cooling water temperature at Heater 1(z = 0.07 m), adiabatic(z = 0.23 m), and condenser section(z = 0.39 m). As can be seen in this figure, as the temperature of the cooling water increases, the temperatures at the three locations increases with a same rate.

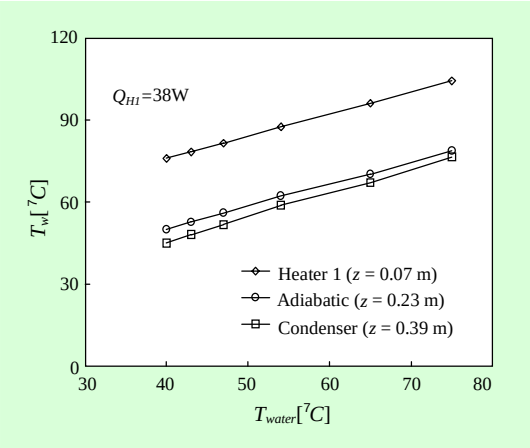


**Fig. 3.** Wall temperature profile with cooling water temperature.

**Table 2.** Test matrix.

| Case | Heater 1 | Heater 2 | Total |
|---|---|---|---|
| 1 | 29 W | 29 W | 58 W |
| 2 | 29 W | 38 W | 67 W |
| 3 | 29 W | 47 W | 76 W |
| 4 | 38 W | 29 W | 67 W |
| 5 | 38 W | 38 W | 76 W |
| 6 | 38 W | 47 W | 85 W |
| 7 | 47 W | 29 W | 76 W |
| 8 | 47 W | 38 W | 85 W |
| 9 | 47 W | 47 W | 94 W |

This means the heat pipe under test is operating normally in the range of 40 °C to 75 °C of cooling water. Based on this result, the temperature of cooling water was maintained at 45 °C throughout the experiment.

Table 2 shows the nine cases of experiment in the present study to optimize the heat distribution on two heaters. The heat input range was from 29 W to 47 W at each heater, consequently, total heat imposed on the heat pipe was a minimum of 58 W and a maximum of 94 W. It was observed that there was no operating failures such as a dry-out in this heat input range.

Wall temperature profiles along the axial direction for Case 1, Case 4, and Case 6 are shown in Figs. 4-6, respectively. The tempera-ture profiles predicted by the numerical modeling are also shown in the same figures, which show a relatively good agreement with experimental data except two locations, those are, at the end of Heater 1(z = 0.1 m) and at the adiabatic section between heaters(z = 0.11 m). The deviation at these two locations was about 15 % compared to the difference between the highest temperature at the heater and the lowest temperature at the condenser section. It is interesting to note that the temperature at Heater 1 is always higher than the predicted value, while it is always lower at the adiabatic section. This implies that the heat pipe under the present experiment has a lower performance than the modeled one. In general, it is known that the heat pipe performance is worse than those predicted by theoretical model [14]. The reason for this is because the wick structure, specially multi-layered metal screen mesh is not completely attached to the wall surface and to each layer, so that the return of working fluid may not be uniform. The temperature deviation in the present study seems to be resulted from the similar reason.

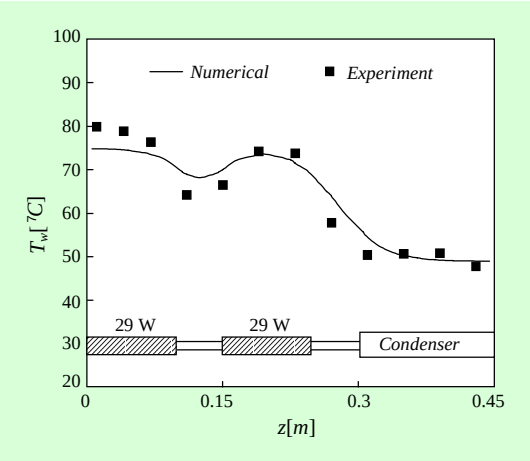


**Fig. 4.** Wall temperature profile with axial location for Case 1.

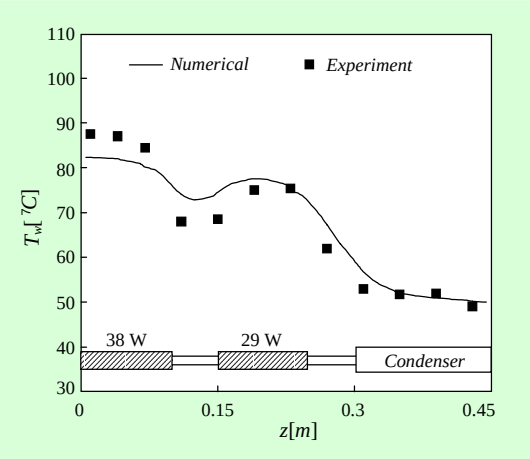


**Fig. 5.** Wall temperature profile with axial location for Case 4.

As shown in Figs. 4 and 5, it seems to be natural that the temperature is higher at Heater 1 than in Heater 2 due to the higher or same amount of heat input to the Heater 1 compared to that for Heater 2. However, it is noticeable that the temperature at Heater 1 is still higher than that at Heater 2 in spite of the higher heat input at

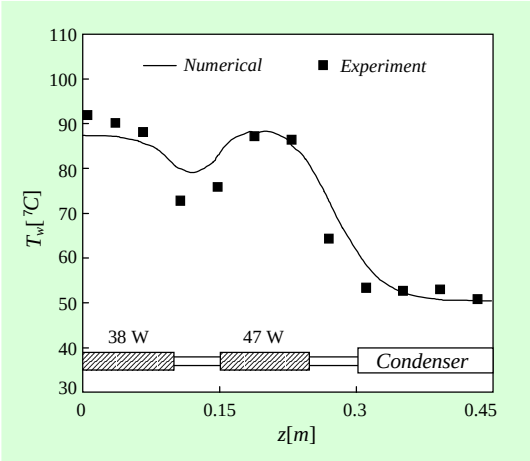


**Fig. 6.** Wall temperature profile with axial location for Case 6.

Heater 2 as shown in Fig. 6. As Faghri and Buchko [4] concluded in their experiment, the higher heat load can be carried in the evaporator located closer to the condenser section due to the better return of working fluid as well as the axial conduction through the wall and wick. This argument can be applicable to the present study.

To evaluate the thermal performance of the copper-water heat pipe used in the present study, it would be valuable to compare the wall temperatures corresponding to the heat input. The experimental wall temperature profiles for the total heat input of 76 W(Case 3, Case 5, and Case 7, respectively) are shown together in Fig. 7. In this figure, $Q_{H1}$ means the heat input at Heater 1 and $Q_{H2}$ at Heater 2. Considering the same amount of the total heat input, it is interesting that the wall temperatures appear differently according to the heat distribution. The maximum temperature difference between the heater and

the condenser section was observed in Case 7(47 W at Heater 1 and 29 W at Heater 2), while the minimum temperature difference was observed in Case 3(29 W at Heater 1 and 47 W at Heater 2). This implies that the maximum heat transport capability can be increased by the optimum distribution of the heat input, while maintaining the maximum allowable temperature which is a major thermal parameter in equipment placement, within the desired limit.

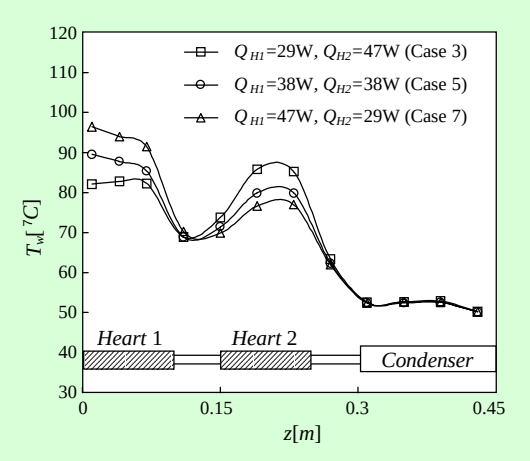


**Fig. 7.** Comparison of wall temperatures for total heat input 76 W. (Case 3, Case 5, and Case 7)

Among the nine cases listed in Table 2, the temperature was higher at Heater 2 than at Heater 1 in Case 3 only. The temperatures were higher at Heater 1 in all other cases although there were two more cases where the amount of heat input was larger at Heater 2 than at Heater 1. Again, it should be emphasized that the optimum heat distribution is important to maintain the outer wall temperature within the designed limit.

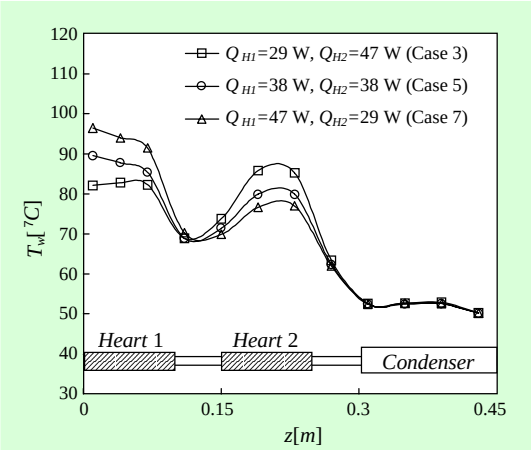


**Fig. 8.** The ratio of temperature increase *vs.* the ratio of heat input between Heater 1 and Heater 2.

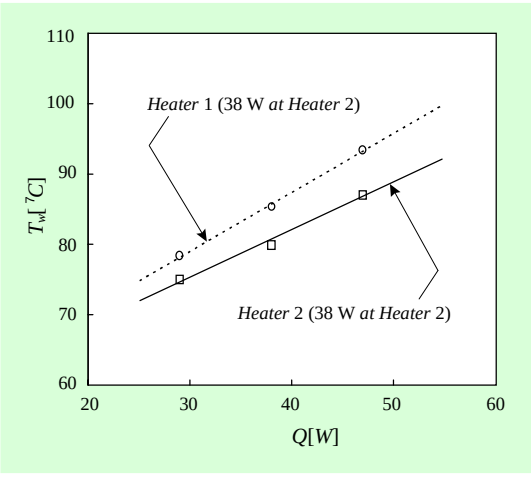


**Fig. 9.** Wall temperature increase with heat input.

The ratio of the temperature increase versus the ratio of the heat input between Heater 1 and Heater 2 of the heat pipe obtained from the present experiment is shown in Fig. 8. In this figure, $T_{H1}$, $T_{H2}$, and $T_C$ are the mean temperatures at Heater 1, Heater 2, and condenser, respec-

tively. To extend this result, it would be valuable to formulate the correlations between the heat input ratio and mean temperature increase ratio. The solid line in Fig. 8 is expressed as (14), which can be used to predict the mean temperature difference between two locations based on the heat ratio in other configuration of a heat pipe.

$$\left(\frac{T_{H1}-T_C}{T_{H2}-T_C}\right) = 0.715\left(\frac{Q_{H1}}{Q_{H2}}\right) + 0.47 \quad (14)$$

The information on the mean temperature increase at the outerwall with respect to the heat input would be useful for optimum heat distribution. Fig. 9 shows the results on the wall temperature increase with heat input obtained from the present study. The trend of the temperature at Heater 1 with a fixed heat input of 38 W at Heater 2 is drawn with a dashed line and the temperature trend at Heater 2 with a fixed heat input of 38 W at Heater 1 is drawn with a solid line in the figure. It was found that $0.8°C$ increased per watt at Heater 1 and $0.7°C$ increased per Watt at Heater 2.

## V. CONCLUSIONS

The performance of a heat pipe with two heat sources has been investigated for the optimum placement of satellite equipment. The prediction of the temperature profile for the heat pipe is performed by a numerical modeling and verified by the experiment with a 0.45 m copper-water heat pipe. The temperature profiles by the numerical model and the experiment are presented for nine different heat distributions on two heaters. In addition, a correlation for the ratio of the temperature increase versus the ratio of the heat input at two heaters as well as rate of the temperature increase with the heat input are proposed for the optimum placement of heat sources for this particular heat pipe. The results show that the temperature profile at the outer wall can be controlled by the optimum distribution of heat sources. Larger heat can be carried by locating the higher heat dissipating equipment closer to the condenser section, while maintaining the maximum temperature controlled.

The numerical methodology and the correlations in the present study can be easily extended to predict the performance of the heat pipe with different thermal configurations.

## REFERENCES

[1] F. Doran, "Heat pipe research and development in the Americas," *Heat Recovery Systems and CHP*, vol. 9, no. 1, pp. 67-100, 1989.

[2] Y. Lee, I. Pioro, and H. J. Park, "An experimental study on a plate type two-phase closed thermosyphon," Paper S-1-3, $4^{th}$ International Heat Pipe Symposium, Tsukuba, May, 1994.

[3] N. J. Gernert, "Analysis and performance evaluation of heat pipes with multiple heat sources," AIAA/ASME $4^{th}$ Joint Thermophysics and Heat Transfer Conference, AIAA-86-1360, 1986.

[4] A. Faghri and M. Buchko, "Experimental and numerical analysis of low-temperature heat pipes with multiple heat sources," *Journal of Heat Transfer*, vol. 113, pp. 728-734, 1991.

[5] J. H. Jang, A. Faghri, W. S. Chang, and E. T. Mahefkey, "Mathematical modeling and analysis of heat pipe start-up from the frozen state," *Journal of Heat Transfer*, vol. 112, pp. 586-594, 1990.

[6] Y. Cao and A. Faghri, "Transient two-dimensional compressible analysis for high temperature heat pipes with a pulsed heat input," *Numerical Heat Transfer*, Part A, vol. 18, pp. 483-502, 1990.

[7] J. H. Park and J. H. Lee, "A numerical study on the heat pipe with switched heat source and sink for space application," *ASME HTD-Vol. 329, National Heat Transfer Conference*, vol. 7, pp. 109-116, 1996.

[8] M. M. Chen and A. Faghri, "An analysis of the vapor flow and the heat conduction through the liquid-wick and pipe wall in a heat pipe with single or multiple heat source," *Int. Journal of Heat Mass Transfer*, vol. 33, no. 9, pp. 1945-1955, 1990.

[9] W. J. Bowman and J. Hitchcock, "Transient compressible heat-pipe vapor dynamics," *Proc. of 25th ASME National Heat Transfer Conference*, vol. 1, pp. 361-365, 1988.

[10] P. D. Dunn and D. A. Reay, *Heat Pipes*, 4th Ed., New York: Pergamon, pp. 45-60, 1994.

[11] E. N. Ganic, J. P. Hartnett, and W. M. Rohsenow, "Basic concepts of heat transfer," in *Handbook of Heat Transfer Fundamentals*, Rohsenow *et al.*, Eds., New York: McGraw-Hill, 1985.

[12] A. Faghri, *Heat Pipe Science and Technology*. Taylor & Francis, pp. 136-138, pp. 268-281, 1995.

[13] H. I. Rosten and D. B. Spalding, *Phoenics Training Course Notes CHAM TR/300*, CHAM, 1990.

[14] J. H. Boo and S. H. Jin, "Development of a computer code for the performance analysis and design of low-temperature heat pipes having screen wick," *Trans. of KSME*, vol. 17, no. 3, pp. 698-709, 1993.

**Jong Heung Park** received his B.S., M.S., and Ph.D. degrees in Mechanical Engineering from Hanyang University in 1982, in 1990, and in 1997, respectively. He had worked on the thermal design, mechanical design and evaluation of the electronic system such as TDX, TICOM, and SMX. He joined the Koreasat Program for two and half years at MMS(Matra Marconi Space), U.K. and LMAS(Lockheed Martin Astro Space), U.S.A. He is currently working on the mechanical and thermal design of the transponder system for the communication satellite.